J Electr Eng Technol Vol. 8, No. 3: 393-401, 2013
http://dx.doi.org/10.5370/JEET.2013.8.3.393

ISSN(Print) 1975-0102
ISSN(Online) 2093-7423

Operation Strategy of Cheju AC Network Included Multi-Infeed HVDC System

Chan-Ki Kim* and Gilsoo Jang†

Abstract – This paper deals with the operation strategy of the Cheju AC network included MIHVDC system (Multi-Infeed HVDC system). In case that where several HVDC systems are located in the vicinity of each other, there are interactions between the different HVDC systems in such network configurations. The interactions which could be generated in multi-infeed HVDC are voltage stability, power stability and inertia stability, to analyze such systems in a systematic way to ensure that there are no risks of adverse interactions is very important. The developed method until now to analyze MIHVDC interaction is extended from MAP(Maximum Available Power) method for analyzing the power stability of the single-infeed HVDC system, this method is to solve the eigenstructure using the identified factors influencing the interactions. Finally, the algorithms which are introduced in this paper, to determine the operation strategy are applied to Cheju island network which is supplied by two HVDCs.

Keywords: MIHVDC(Multi-Infeed HVDC), Power stability, Voltage stability, Inertia stability

1. Introduction

Cheju island of Korea is located at the southern of Korea Peninsular. Because Cheju's main industry is tourism, additional installation of thermal power plant is not suitable from the viewpoint of environment. Therefore, two HVDCs were constructed in 1997 and 2012 each other.

Because Cheju network is connected by HVDCs and have less thermal power plants, relatively weak system from viewpoint of the stability. These conditions can cause the stability problems, which termed **"Multi-infeed HVDC instability"**, is related to voltage stability, power stability and frequency stability (or inertia stability).

The object of this paper is to determine the operation strategy of Cheju network, without stability problems.

Single HVDC converter feeding into an AC system is generally termed as a single-infeed HVDC system. When the AC system is relatively weak, the interconnected AC/DC system brings concomitant problems relating to voltage and power instability. Therefore until now, much research focus had been on problems of such nature for the single-infeed HVDC system. As the application of HVDC systems continues to develop, situations also arise with two or more HVDC converters feeding into AC system locations that are electrically in close proximity. Such systems, termed as multi-infeed HVDC systems, supply to the motivation to study phenomenons concerning interactions between the various AC and DC systems, particularly when the AC system is again relatively weak.

From the results of many research, analytical techniques developed for and results accrued from the single-infeed HVDC system case are valid for multi-infeed HVDC system scenarios and the interaction phenomena and associated problems for the multi-infeed HVDC system are closely related to the single-infeed HVDC system case [1].

Main approaches to analyze the voltage and power stability of weak single-infeed AC/DC interconnections had been reported. The power stability, known as the Maximum Power Curve (MPC) method, is based on the concept of Maximum Available Power(MAP) and was first introduced by Ainsworth [2]. The Voltage stability, known as the Voltage Stability Factor (VSF) method, is based on the concept of voltage sensitivity and was presented by Hammad [3]. Essentially, both approaches use sensitivity of system states to small changes in controlling system quantities, as a measure of system stability.

Additionally, the commutation failure vulnerability of multi-infeed HVDC converters to AC side faults is analyzed by Gole. Faults in multi-infeed systems can cause commutation failure events in the nearby local converter or concurrently in both converters. "Commutation Failure Immunity Index (CFII)" is calculated for multi-infeed systems with different ratings. CFII can be used to calculate MIESCR (Multi-Infeed Effective Short Circuit Ratio).

In the islanded AC network, the role of generators is very important. Turbine generators in an AC system represent a large rotating mass which means mechanical energy storage system. Their inertia ensures that an AC system does not collapse due to system faults. During a fault, a balance of power between the load consumption

† Corresponding Author: School of Electrical Engineering, Korea University, Korea. (gjang@korea.ac.kr)
* Korea Electric Power Research Institute, Daejon, Korea. (ckkim@kepri.re.kr)
Received: July 1, 2012; Accepted: January 21, 2013

and generation is not maintained. The mechanical inertia of turbine generator set ensures that its speed and the frequency of the system has not changed substantially. If the greater part of the power is brought into an AC system by HVDC system, HVDC inverter must be provided with a rotating machines (synchronous compensator or generators) having adequate inertia to maintain the frequency and voltage to an acceptable level during system faults [4, 5].

Consequently, the algorithms which was discussed in this paper, is applied to Cheju island network to maintain AC network safe.

2. Background for the Stability of Multi-Infeed HVDC

2.1 Multi-infeed HVDC system

Fig. 1 shows the simplified single-infeed HVDC system. The SCR, short-circuit ratio, is defined as Eq.(1) and the ratio between the voltage change, ΔU, and a reactive power Injection, ΔQ, causing this voltage change was used as a stability indicator, called voltage stability factor, VSF, defined as Eq. (2);

$$SCR = \frac{1}{Z} \tag{1}$$

$$VSF = \frac{\Delta U}{\Delta Q} \tag{2}$$

The voltage stability of a power system was closely related to the properties of the power-flow Jacobian, so that if the Jacobian was close to becoming singular this would indicate a power system with small voltage stability margin. From Fig. 1, the Jacobian matrix shown in Eq. (3) can be derived. In Eq. (3), In order to decouple the bus angles from the bus reactive power incremental change equations in Eq. (3), supposing to set ΔP=0, i.e., no active power injections, Eq. (4) can be calculated.

$$\begin{bmatrix} \Delta P \\ \Delta Q \end{bmatrix} = \begin{bmatrix} J_{P\delta} \, J_{PU} \\ J_{Q\delta} \, J_{QU} \end{bmatrix} \begin{bmatrix} \Delta \delta \\ \Delta U \end{bmatrix} \tag{3}$$

$$\frac{\Delta U}{U} = J_R^{-1} \Delta Q \tag{4}$$

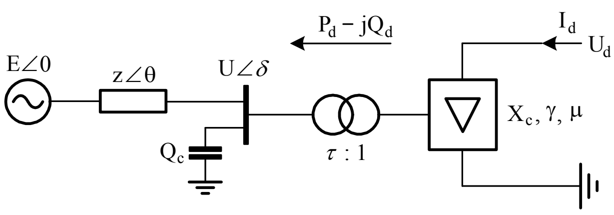

Fig.1. Simplified model of the HVDC system connected to AC power system

Where, $\Delta Q = J_R \frac{\Delta U}{U}$, $J_R = J_{QU} - J_{Q\delta} J_{P\delta}^{-1} J_{PU}$

The relation between bus reactive power changes and bus voltage magnitude changes is shown in Eq. (4) and it is easily seen that this equation constitute a generalization of VSF, and J_R^{-1}, is thus the multi-dimensional equivalent of VSF. The criterion of voltage stability is that all eigenvalues of J_R, are positive, The meaning of this is that the incremental change in bus voltage magnitude is in phase with the incremental change in reactive power, increasing bus voltage magnitude when positive reactive power increments are applied and vice-versa. This physically corresponds to voltage stable situations.

When studying complex systems such as a multi-infeed HVDC system interconnected with a large AC network, it is often essential to abstract a simplified model from the complex system while retaining the underlying topological structure. This would conceivably preserve the fundamental system response, behaviour, and properties of the original system but now making it easier to study, expose, and elucidate them. At the same time, since this work is a generalization of the single-infeed HVDC system case, there is strong motivation to use a model analogous to the single-infeed HVDC system apart from being representative of the multi-infeed HVDC system, so that parallels between them can be drawn. In this model, one or both converters could be rectifiers or inverters operating in a variety of control modes, e.g. constant gamma/constant power, constant gamma/constant current, etc. Fig. 2 shows the simplified model of the multi-infeed HVDC system connected to AC power system.

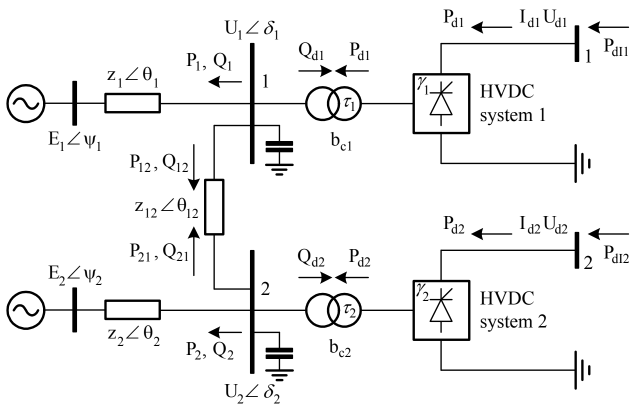

Fig. 2. Simplified model of the multi-infeed HVDC system connected to AC power system

2.1.1 MIESCR(multi-infeed effective short circuit ratio) and commutation failure

The Multi-Infeed Interaction Factor (MIIF) is a parameter for estimating the degree of voltage interaction between two converters. The MIIF from converter 1 to converter 2 is essentially the ratio of voltage drops at the two converter busses following a 1% voltage reduction at the ac busbar of converter 1 caused by a three-phase balanced inductive fault.

As the effective short circuit ratio is an indicator of the performance of a given converter without any other converter in operation, the Thevenin impedance is measured looking into the AC network from the converter's AC bus. The other converter is considered to be blocked in this calculation. Thus the ESCR for the i-th converter is given by Eq. (6).

$$MIIF_{j,i} = \frac{\Delta V_j \%}{1\% voltagedropinV_i} \tag{5}$$

$$MIIESCR_i = \frac{SCR_i - Q_{fi}}{P_{dci} + \sum_j MIIR_{ji} \cdot P_{dcj}} \tag{6}$$

Earlier approaches to quantify the susceptibility of the converter to commutation failure to calculate the maximum permissible balanced voltage drop on the converter's AC busbar. If the voltage dropped by more than this amount, commutation failure was presumed to occur.

$$\Delta V = 1 - \frac{I_d^{'}}{I_d} \frac{(I_d / I_{dFL}) \cdot X_{cpu}}{(I_d / I_{dFL}) \cdot X_{cpu} + \cos\gamma_0 - \cos\gamma} \tag{7}$$

where, I_d : prefault DC current, $I_d^{'}$: postfault DC current, I_{dFL} : nominal current, X_{cpu} : transformer %impedance, γ : operation extinction angle, $\gamma 0$: absolute minimum extinction angle which commutation fails

The analysis of commutation failure in multi-infeed HVDC systems indicates that the local commutation failures are essentially affected only by the local short circuit ratio, with the immunity level increasing as local ESCR increases. For MIIF < 0.15, commutation failure of the remote converter is not affected by the local converter operation. For MIIF > 0.6, a commutation failure causing AC fault on local bus will cause a concurrent commutation failure on the remote converter as well. MIIF is very important on independent multi-infeed HVDC like Cheju island, the reason is because MIIF decides a concurrent commutation failure, which affects power interruption and power interruption is related to the overvoltage, inertia and reliability of AC system with HVDC.

2.1.2 Voltage stability

The analysis developed above is applicable to all systems where the equations and relations determining the behavior can be linearized to a form as in (3). Therefore, the Jacobian matrix of the dual-inverter HVDC system after eliminating the Thevenin equivalent source buses of AC subsystems 1 and 2 can be written as Eq. (8). The nomenclature used in Fig. 2 is similar to that of the single-infeed HVDC system of Fig. 1, but now with the subscript 1 and 2 denoting the correspondence of each parameter with the constituent AC/DC subsystem 1 and 2, respectively.

$$J_{p\delta} = \begin{bmatrix} \frac{\partial \Delta P_{t1}}{\partial \delta_1} & \frac{\partial \Delta P_{t1}}{\partial \delta_2} \\ \frac{\partial \Delta P_{t2}}{\partial \delta_1} & \frac{\partial \Delta P_{t2}}{\partial \delta_2} \end{bmatrix} \quad J_{PU} = \begin{bmatrix} U_1 \frac{\partial \Delta P_{t1}}{\partial U_1} & U_2 \frac{\partial \Delta P_{t1}}{\partial U_2} \\ U_1 \frac{\partial \Delta P_{t2}}{\partial U_1} & U_2 \frac{\partial \Delta P_{t2}}{\partial U_2} \end{bmatrix}$$
$$J_{Q\delta} = \begin{bmatrix} \frac{\partial \Delta Q_{t1}}{\partial \delta_1} & \frac{\partial \Delta Q_{t1}}{\partial \delta_2} \\ \frac{\partial \Delta Q_{t2}}{\partial \delta_1} & \frac{\partial \Delta Q_{t2}}{\partial \delta_2} \end{bmatrix} \quad J_{QU} = \begin{bmatrix} U_1 \frac{\partial \Delta Q_{t1}}{\partial U_1} & U_2 \frac{\partial \Delta Q_{t1}}{\partial U_2} \\ U_1 \frac{\partial \Delta Q_{t2}}{\partial U_1} & U_2 \frac{\partial \Delta Q_{t2}}{\partial U_2} \end{bmatrix} \tag{8}$$

It is more meaningful to specify the Effective Short Circuit Ratio according to base MVA of individual constituent AC/DC subsystems, it is more convenient to specify impedances in per unit on the common MVA base. Power Base Ratio, PBR, as the ratio of DC power ratings of HVDC subsystems 2 and 1 is given by;

$$PBR = \frac{P_{dn2}}{P_{dn1}}, \quad ESCR1 = \frac{1}{z_1} - b_{c1},$$
$$ESCR2 = \frac{1}{PBR}\left(\frac{1}{z_2} - b_{c2}\right) \tag{9}$$

where, z_1, z_2, b_{c1} and b_{c2} are in per unit on a base MVA and P_{dn1} base MVA and U_R base voltage.

The elements of J_{tR} of Eq.(10) are functions of a_1, a_2, a_3 and A for given system loading conditions. Also, a_1, a_2, a_3 and A are all algebraic functions of ESCR1, ESCR2, PBR and z_{12}. In principle, the components of J_{tR} in Eq.(10) can be calculated by applying the eigenvalue decomposition theory, analytic form of its eigenvalues (in terms of ESCR1, ESCR2, PBR, z_{12}) could also be obtained.

$$\Delta Q_t = \begin{bmatrix} \Delta Q_{t1} \\ \Delta Q_{t2} \end{bmatrix}, \quad \frac{\Delta U_t}{U_t} = \begin{bmatrix} \frac{\Delta U_{t1}}{U_{t1}} \\ \frac{\Delta U_{t2}}{U_{t1}} \end{bmatrix}, \quad J_{tR} = \begin{bmatrix} J_{11} & J_{12} \\ J_{21} & J_{22} \end{bmatrix} \tag{10}$$

Where,

$$J_{11} = a_1 - 2Q_{d1} + U_1 \cdot \frac{\partial Q_{d1}}{\partial U_1} - \frac{1}{A}\left[(P_{d1}a_2 + P_{12}a_3)\left(P_{d1} - U_1 \cdot \frac{\partial Q_{d1}}{\partial U_1}\right) + P_{12}(P_{d1}a_3 + P_{12}a_1)\right]$$

$$J_{12} = a_3 - \frac{1}{A}\left[P_{12}(P_{d1}a_2 + P_{12}a_3) - (P_{d1}a_3 + P_{12}a_1)\left(P_{d1} - U_1 \cdot \frac{\partial Q_{d2}}{\partial U_2}\right)\right]$$

$$J_{21} = a_3 - \frac{1}{A}\left[P_{12}(P_{12}a_3 - P_{d2}a_1) + (P_{12}a_2 - P_{d2}a_3)\left(P_{d1} - U_1 \cdot \frac{\partial Q_{d1}}{\partial U_1}\right)\right]$$

$$J_{22} = a_2 - 2Q_{d2} + U_2 \cdot \frac{\partial Q_{d2}}{\partial U_2}$$

$$-\frac{1}{A}\left[(P_{d2}a_1 - P_{12}a_3)\left(P_{d2} - U_2 \cdot \frac{\partial Q_{d2}}{\partial U_2}\right) + P_{12}(P_{12}a_2 + P_{d2}a_3)\right]$$

$$J_{22} = a_2 - 2Q_{d2} + U_2 \cdot \frac{\partial Q_{d2}}{\partial U_2}$$

$$-\frac{1}{A}\left[(P_{d2}a_1 - P_{12}a_3)\left(P_{d2} - U_2 \cdot \frac{\partial Q_{d2}}{\partial U_2}\right) + P_{12}(P_{12}a_2 + P_{d2}a_3)\right]$$

$$a_1 = Q_{d1} + ESCR1 \cdot U_1^2 + \frac{U_1^2}{z_{12}} \quad ,$$

$$a_2 = Q_{d2} + PBR \cdot ESCR2 \cdot U_2^2 + \frac{U_2^2}{z_{12}}$$

$$a_3 = -\frac{U_1 U_2}{z_{12}}\cos(\delta_1 - \delta_2)\,, \quad A = a_1 a_2 - a_3^2$$

For an integrated AC/DC power system the HVDC converter equations have to be incorporated and this is possible by treating the PQ load of the HVDC converter as voltage dependant active and reactive power loads, where the voltage dependence is determined by the control mode of the converter, i.e., constant power or current, constant γ, etc. The elements of the Jacobian matrix for different control modes can be calculated following as :

For the case of constant power control mode

$$\frac{\partial P_{di}}{\partial U_i} = 0\,, \quad \frac{\partial Q_{di}}{\partial U_i} = \frac{2}{U_i}\left[Q_{di} - P_{di}\tan(\gamma_i + \mu_i)\right] \tag{11}$$

For the case of constant current control mode

$$\frac{\partial P_{di}}{\partial U_i} = \frac{3\sqrt{2}}{\pi U_i} I_{di}\cos\gamma\,,$$

$$\frac{\partial Q_{di}}{\partial U_i} = \frac{2}{U_i}\left[Q_{di} - P_{di}\frac{\sin(\gamma_i + \mu_i)}{\cos\alpha_i + \cos(\alpha_i + \mu_i)}\right] \tag{12}$$

The eigenvalues are found from the characteristic equation of the Reduced-Jacobian matrix of (10), and its values must be positive for voltage stable systems. This leads to the following criteria.

$$\det(J_{tR}) = (J_{11}J_{22} - J_{12}J_{21}) > 0 \tag{13}$$

$$J_{11} > 0\,, \quad J_{22} > 0 \tag{14}$$

Where, $\det(J_{tR})$ denotes the determinant of the Reduced-Jacobian matrix.

2.1.3 Power stability

In the Maximum Power Curve (MPC) method, the inverter DC power, P_d, is graphically derived as a function of the direct current, I_d with the inverter operating in constant γ control mode. Starting from nominal conditions, U, U_d, I_d at 1 [p.u.], the AC Thevenin equivalent voltage magnitude, E, is computed and subsequently held constant, when the MPC is computed. Typical curve is shown in Fig.3. From the MPC, the Maximum Available Power (MAP) is defined as the

DC power corresponding to a direct current, I_{MAP} as Eq. (15).

$$\frac{dP_d}{dI_d} = 0 \tag{15}$$

Beyond I_{MAP} DC power actually decreases with further increase in direct current. Such phenomenon corresponds with unstable system behavior. Thus, the MAP determines the power stability limit of the interconnected AC/DC system. The MAP is related to the short-circuit ratio(SCR).

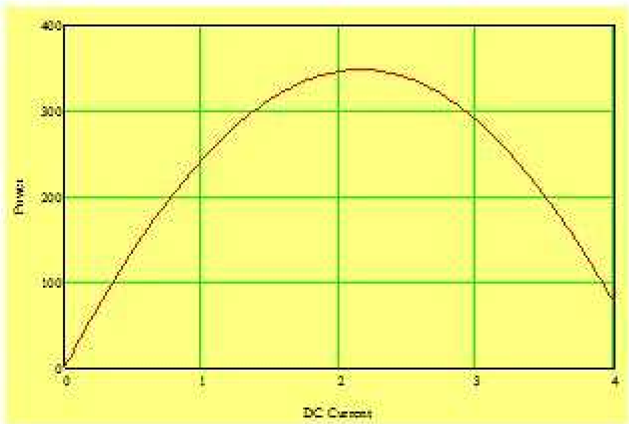

Fig. 3. MPC for single-infeed HVDC system

Under nominal conditions, if the actual initial operating point corresponds to the MAP, then the ESCR is said to be critical, CESCR. If the angle of the AC Thevenin equivalent impedance is assumed to be 90 degrees, to simplify analysis, it can be shown that;

$$CESCR = \frac{1}{U^2}\left[P_d\cot\left(\frac{\pi}{4} - \frac{\gamma + \mu}{2}\right) - Q_d\right] \tag{16}$$

The linearized system power flow equations of HVDC system in matrix notation, are given by;

$$\begin{bmatrix} \Delta P_{DC} \\ \Delta P_{AC} \\ \Delta Q_{AC} \end{bmatrix} = \begin{bmatrix} J_{DI}\, J_{D\delta}\, J_{DU} \\ J_{PI}\, J_{P\delta}\, J_{PU} \\ J_{QI}\, J_{Q\delta}\, J_{QU} \end{bmatrix} \begin{bmatrix} \Delta I_d \\ \Delta\delta \\ \dfrac{\Delta U}{U} \end{bmatrix} \tag{17}$$

where, ΔP_{DC} : DC power incremental at inverter DC bus

ΔP_{AC} and ΔQ_{AC}: AC active and reactive power incremental change respectively, at inverter AC bus
ΔI_d: vector of incremental direct currents of the inverters.
$\Delta\delta$: vector of incremental voltage angle of the inverter AC buses
U/U: vector of incremental voltage magnitudes of the inverter AC buses

From Eq. (17), if there are no active or reactive power injections at the inverter AC buses, we may assume that ΔP_{AC} and ΔQ_{AC} are zero. And ΔP_{DC} is simplified following as :

$$\begin{bmatrix} \Delta P_{DC} \\ 0 \\ 0 \end{bmatrix} = \begin{bmatrix} J_{DI}\, J_{D\delta}\, J_{DU} \\ J_{PI}\, J_{P\delta}\, J_{PU} \\ J_{QI}\, J_{Q\delta}\, J_{QU} \end{bmatrix} \begin{bmatrix} \Delta I_d \\ \Delta\delta \\ \dfrac{\Delta U}{U} \end{bmatrix}, \quad \Delta P_{DC} = J_{MPC}\Delta I_d \quad (18)$$

From Eq. (18), the DC power-DC current Reduced Jacobian matrix is obtained following as :

$$J_{MPC} = \left[J_{DI} - J_{DU} J_{R1}^{-1} J_{R2} \right] \quad (19)$$

Where $J_{R1} = J_{QU} - J_{Q\delta}$, $J_{R2} = J_{QI} - J_{Q\delta} J_{P\delta}^{-1} J_{PI}$

To investigate the power stability of the multi-infeed HVDC system, allowing only single degree of freedom for the direct currents to vary, constraining the others as constant parameters is proper. This is equivalently expressed as Eq. (20)

$$\left.\frac{\Delta P_{DCi}}{\Delta I_{di}}\right|_{\Delta I_{dj}=0} = J_{MPCii}, \quad i,j = 1,2|_{i\neq j}, \quad (20)$$

When J_{MPCii} becomes zero, Eq. (20) is similar to the single-infeed HVDC case, the modified equation may also be used to define the power stability of the multi-infeed HVDC system, as the operating point where;

$$\left.\frac{\Delta P_{DCi}}{\Delta I_{di}}\right|_{\Delta I_{dj}=0} = 0, \quad i,j = 1,2|_{i\neq j} \quad (21)$$

When the multi-infeed HVDC system of Fig. 2 is decoupled, by allowing the coupling impedance, z_{12} , to have an arbitrarily large value, it can be shown analytically that J_{MPC} reduces to a diagonal matrix, whose diagonal element is given by Eq. (22). Therefore, In order to satisfy the power stability boundary condition, J_{MPCii} becomes zero at the root of the diagonal element in Eq. (22) for the single-infeed MPC. Thus, when the multi-infeed HVDC system is decoupled, the MIMPC (Multi-Infeed MPC) method reduces to its single dimensional equivalent which is the MPC method for the single-infeed case.

$$\begin{aligned} J_{MPCii} &= ESCR_i^2 U_i^4 + 2\left[Q_{di} - P_{di}\tan(\gamma_i + \mu_i)\right] ESCR_i U_i^2 \\ &\quad -(P_{di}^2 + Q_{di}^2) + 2Q_{di}\left[Q_{di} - P_{di}\tan(\gamma_i + \mu_i)\right] \end{aligned} \quad (22)$$

2.1.4 Effective inertia

The inertia constant in AC network is relative, its value can be changed according to the operating condition of generator. For example, a typical steam turbine-generator system may have an inertia constant H_{rated} based on the generator MVA rating. Assume that a generator operates at some power factor so that the inertia constant H_{real} based on MW rating, can be calculated as Eq. (23).

$$H_{rated} = \frac{H_{rated}}{p \cdot f} \quad (23)$$

Also, since HVDC system has no inertia, the total inertia of AC network is supplied by HVDC system, become less than the inertia constant H_{real} of MW rating. The DC inertia constant, H_{DC} which is the total inertia AC network is infeed by HVDC depends on a number of the rotating machine and the proportion of the power supply infeed by HVDC. The equation solving DC inertia is Eq. (24).

$$\begin{aligned} H_{DC} &= \frac{H_1 \cdot P_{ac1} + H_2 \cdot P_{ac2} \cdots + H_n \cdot P_{acn}}{P_{ac1} + P_{ac2} \cdots + P_{acn} + \sum_{i=1}^{n} HVDC_n} \\ &= \frac{\sum_{i=0}^{n} H_n \cdot P_{acn}}{\sum_{i=0}^{n} P_{acn} + \sum_{i=1}^{n} HVDC_n} \end{aligned} \quad (24)$$

where, H_i : inertia constant of rotating machine, P_{aci} : MW rating of rotating machines, $HVDC_i$: HVDC power

The relationship between change of machine frequency (Δf) and HVDC interruption power (ΔP_{HVDC}) for small changes of frequency can be represented by Eq. (25).

$$\Delta f = \frac{\Delta P_{HVDC} \cdot f_o \cdot \Delta t}{2 \cdot H} \quad (25)$$

where, f_o is the system nominal frequency and H is the conventional inertia constant of the machine expressed in MW-s/MVA of machine capacity and Δt is the total faults clearing time

$$H_{required} = \frac{\Delta P_{HVDC} \cdot f_o \cdot \Delta t}{2 \cdot \Delta f} \quad (26)$$

where, $H_{required}$: the required minimum inertia constant in AC system, ΔP_{HVDC}: the interrupted HVDC power, Δt: total faults clearing time ($\Delta t = \Delta t1 + \Delta t2 + \Delta t3$, $\Delta t1$: faults clearing time(faults persisting time), Δt2: charging time of HVDC cable(or overhead line), Δt3: HVDC recovery time after faults)

Conventionally, since the low-frequency operation of turbine-generator in AC network cause the stress on the blade of turbine, the low-frequency within 5% of the rated frequency of generator is allowed. the allowed value is a kind of the limitation value, Δf in Eq. (26)

From Eq. (26), a number of generator which must be always run is determined by Eq. (27), this generators are called "Must Run Generator".

$$H_{dc} = \frac{N \cdot (H_{ac} \cdot P_{ac})}{P_{HVDC}}, \quad N = \frac{P_{HVDC} \cdot H_{dc}}{H_{ac} \cdot P_{ac}} \tag{27}$$

where, N: a number of Must Run Generator, H_{ac}: inertia of rotating machine, P_{ac}: Generator MVA rating, P_{HVDC}: HVDC power supply infeed

2.1.5 Temporary overvoltage

The term "TOV(Temporary Overvoltage)" in this paper refers to the complete waveform which consists of the fundamental component and the possible superimposed oscillatory component. Changes in the reactive power balance of the AC network initiated by switching, faults or power flow variation produce changes in the operating voltage. Surplus reactive power also can lead to voltage increase. Large disturbance results in temporary overvoltages. The HVDC system always consumes reactive power in the range of 50% to 60% of HVDC transmitted power. The amount consumed depends on the commutation reactance and operating angle. If the SCR is low, a sudden change in the active power (reactive power) or the blocking of HVDC system due to faults (included commutation failures), lead to high temporary overvoltages. The ratio of TOV U_{ov} to nominal voltage U_{norm} is shown in Eq. (28).

$$U_{ov} = U_{norm}\angle\theta_1 + \frac{1}{SCR(p.u)\angle\theta_2} \tag{28}$$

2.2 Case Study for cheju island network

A feature of Cheju island electrical system, which is not connected to other networks by AC transmission lines, is that its mechanical inertia is due to local rotational machine. The effect on frequency is due to the size of that unit relative to the total load and on the amount of spinning reserve in service. The network of Cheju island constitute two bipole HVDC system, several generators and STATCOM (50MVA × 2). The Cheju HVDC system (HVDC #1 and HVDC #2) is used to transfer 400MW from mainland to Cheju island [6]. The scheme is bidirectional and can be used to transfer power from Cheju to Jindo when necessary. The HVDC system comprises two bipoles, the first rated to transmit 200MW (200MW × 2: considered redundancy (N-1)) at 250 kV with a single twelve pulse converter per pole connected via three HVDC cables and one MV DC cable continuously. the second provides the power supplying capability of 300MW (150MW × 2) at 180kV. Totally eight generators in Cheju island are provided to supply the power to AC system and their total SCC (Short Circuit Capacity) is 2124MVA (N.TP (352MVA) × 2+S. CC(450MVA) × 2+C. Diesel (110MVA)

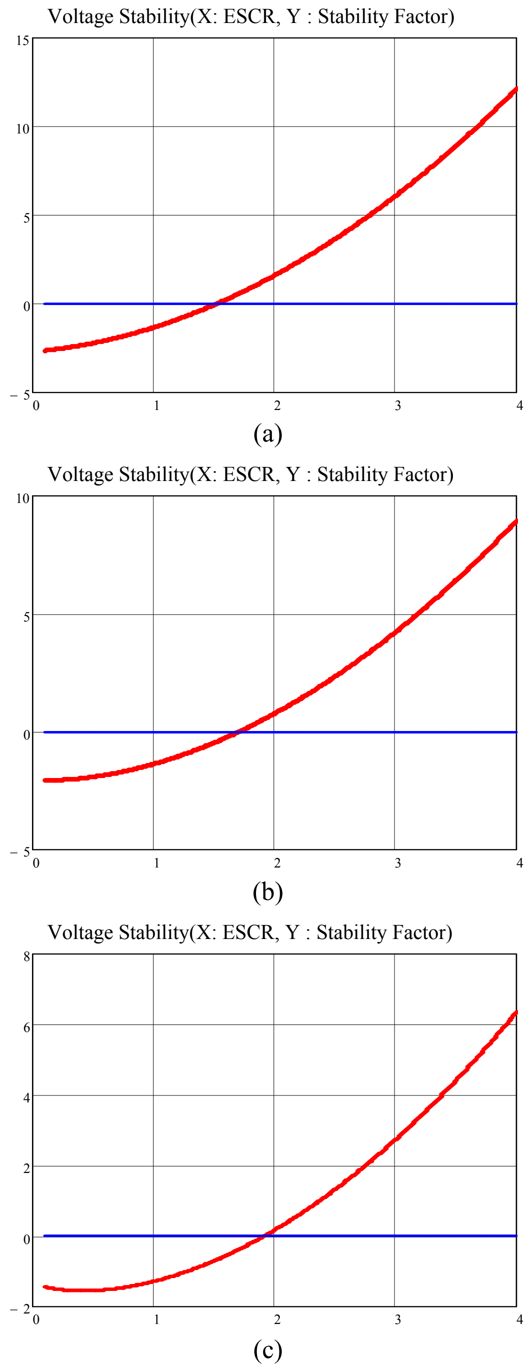

Fig. 4. Voltage stability of MIHVDC(× 2): (a) AC bus voltage 1.0(p.u) : ESCR(2.8(1.4 × 2)); (b) AC bus voltage 0.95(p.u) : ESCR(3.2(1.6 × 2)); (c) AC bus voltage 0.9(p.u) : ESCR(3.6(1.8 × 2))

× 2 + S.C. (150MVA) × 2)

(N.TP : North Cheju Thermal Power Plant, S. CC : South Cheju Combined Complex Power Plant, C. Diesel : Cheju Diesel Power Plant, S.C : Synchronous Compensator.)

The maintaining condition of AC network is case by case every countries, because that each countries have the different characteristics of AC network each other. The required conditions of Cheju island are following as:

* Voltage: Maximum 164kV∓4kV, Minimum 139kV
* Frequency variation: Maximum 5%
* AC network clearing time: 0.1[sec], HVDC recovery time after faults: 0.25[sec], cable charging time: 0.05 [sec]
* HVDC #1: 150MW × 2, Maximum firing angle: 35[deg], Reactive Power: 70% of active power
* HVDC #2: 200MW × 2, Maximum firing angle: 20[deg], Reactive Power: 70% of active power
* Maximum power supplying capacity of HVDC #1 and HVDC #2: 400MW
* Peak Load of Cheju network: 780MW,
* Off-peak Load of Cheju network: 460MW

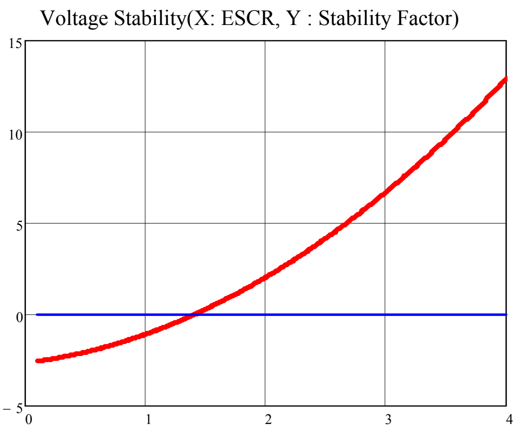

(a)

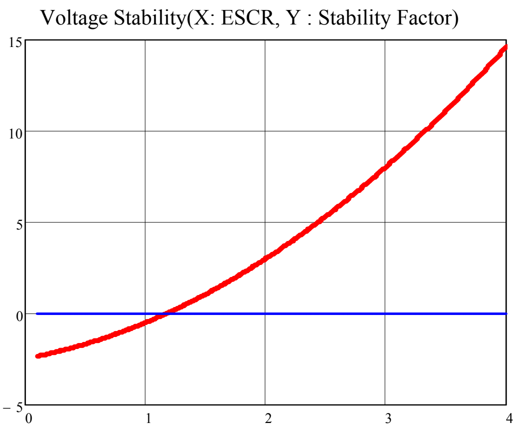

(b)

Fig. 5. Voltage stability of MIHVDC system(× 2): STATCOM :voltage control(100MVA): ESCR (2.4 (1.2 × 2)); STATCOM : reactive power control: ESCR(2.0(1.0 × 2))

* Interaction strength between HVDC #1 and HVDC #2: 0.7
* Cheju STATCOM: 50MVR × 2 (voltage control or reactive control possible)

Therefore, the worst condition of the case study is that

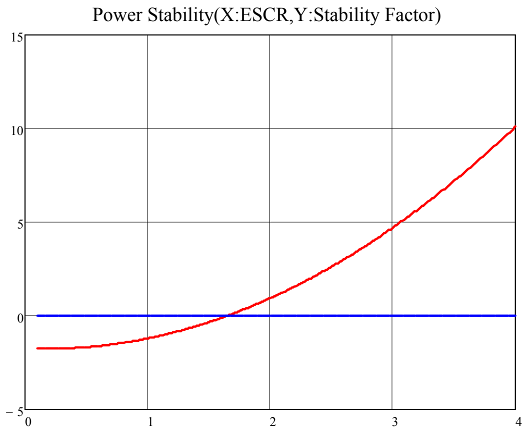

(a)

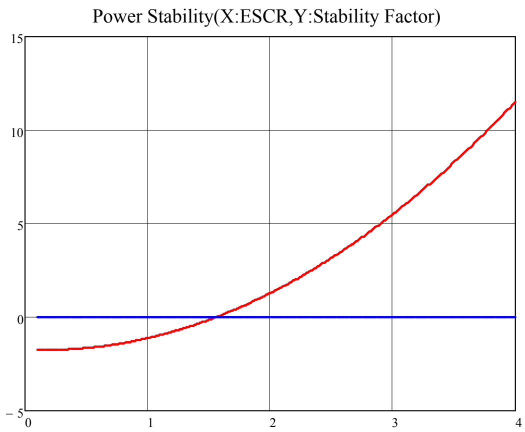

(b)

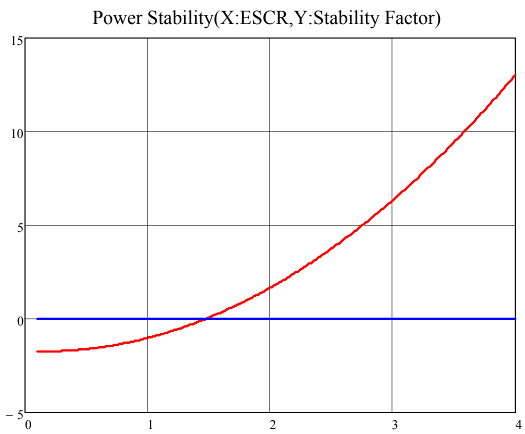

(c)

Fig. 6. Power stability of MIHVDC system(× 2): (a) AC bus voltage 0.9(p.u) : ESCR(3.2(1.6 × 2)); (b) AC bus voltage 0.95(p.u) : ESCR(3.0(1.5 × 2)); (c) AC bus voltage 1.0(p.u) : ESCR(2.8(1.4 × 2))

voltage is 139kV (0.9[p.u]) and fault persisting time is 0.25 [sec]. In order to satisfy the voltage stability, power stability and inertia instability of Cheju island network, that is, to provide the operation strategy of HVDC system of the island system, the strategy which SCR (Short Circuit Ratio) is changed according to HVDC power incremental, is needed. SCR shows the strength of the AC system to HVDC power, it is relative index, which the ratio of SCC of AC network to DC power. SCR variation means the operation condition of the generators.

Fig. 4 shows the voltage stability of MIHVDC system in steady state, a) is in case of voltage 1.0[p.u] and b) in case of voltage 0.95[p.u]. From Fig. 4, ESCR which voltage stability is guaranteed, 2.8 in case a) and 3.6 in case of b). Additionally, Fig. 5 shows the voltage stability results, in case that the simulation condition is the same as Fig. 4(a), Fig. 5(a) is the case that STATCOM is in voltage control mode and (b) in reactive power control mode. From Fig. 5, the stable condition is that ESCR is 2.4 in case of a) and 2 in case of (b).

Fig. 6 shows the power stability of MIHVDC system in steady state, (a) is in case of voltage 0.9[p.u], (b) in case of voltage 0.95[p.u] and (c) in case of 1[p.u]. From Fig. 6, ESCR which power stability is guaranteed, 3.2 in case (a), 3.0 in case of (b) and 2.8 in case of (c).

As Fig. 6 is the simulation results showing power stability range, the stability effects according to the control mode of STATCOM in case of voltage 1.0[p.u] is studied.

In Fig. 6, (a) is the case that STATCOM is in voltage control mode, (b) in reactive power control mode. From Fig. 6, ESCR to meet the stability is 2.8 in case of (a) and 2.4 in case of (b).

Finally, as Table 1 shows the operation strategy of Cheju island network, the operation strategy of generators and HVDC is summarized considering power stability, voltage stability and inertia stability using the contents discussed above.

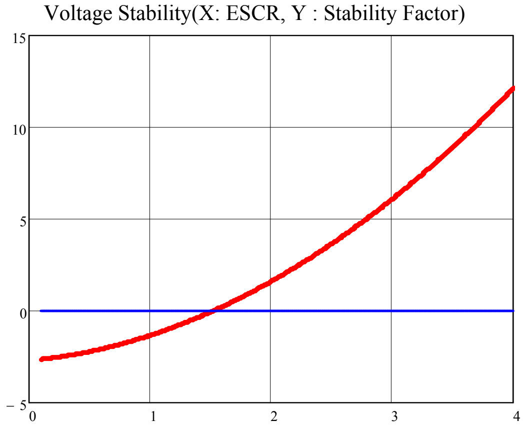

(a)

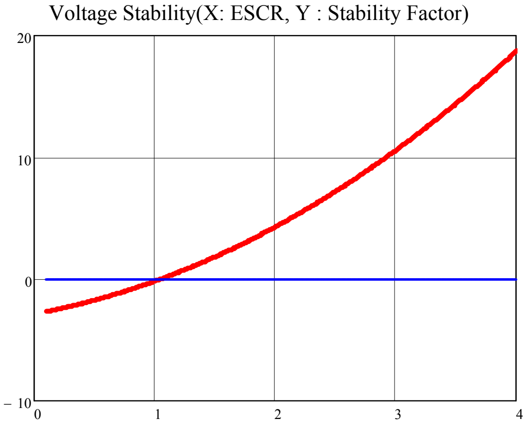

(b)

Fig. 7. Voltage stability of MIHVDC system ($\times$ 2): (a) STATCOM: voltage control(100MVA): ESCR (2.8 (1.4$\times$ 2)); (b) STATCOM : reactive power control : ESCR (2.4(1.2$\times$ 2))

Table 1. Operation strategy of Cheju network in case of peak load

	AC Load	HVDC Load	Gen
Peak Load	780	400	380

Generator	Ser	MVA	Effective	Inertia	SCC
BUKJEJU TP	1	75	60	5.4	352
BUKJEJUTP	1	75	60	5.4	352
NAMJEJU	1	100	90	5.93	450
NAMJEJU	1	100	90	5.93	450
JEJUDP	1	40	40	6.71	110
JEJUDP	1	40	40	6.71	110
SC	1	50	0	1.95	150
SC	1	50	0	1.95	150
MVA			380		2124

Required Inertia	1.282	Present Inertia	3.14
SCR	5.31	ESCR	4.61

5. Conclusion

In case that where several HVDC systems are located in the vicinity of each other, it is evident that interactions between the different HVDC systems occur in such configurations, and it is of importance to analyze such systems in a systematic way to ensure that there are no risks of adverse interactions. The interactions which could be generated in multi-infeed HVDC are voltage stability, power stability and inertia stability. In order to satisfy the voltage stability, power stability and inertia instability of Cheju island network, that is, to provide the operation strategy of HVDC system of the island system, the strategy which SCR(Short Circuit Ratio) is changed according to HVDC power incremental, is needed. SCR (Short Circuit Ratio) shows the strength of the AC system to HVDC power, it is relative index, which the ratio of SCC of AC network to DC power. SCR variation means the operation condition of the generators. As a result, synchronous compensators have to be installed to enhance SCR in Cheju island, instead of the additional generator operation.

Acknowledgements

This work was supported in part by the Human Resources Development of KETEP grant (No. 20114010203010) and by a Korea University Grant.

References

[1] E. Rahimi, etc 4, "Commutation Failure Analysis in Multi-Infeed HVDC Systems", IEEE transactions on power delivery, Vol. 26, No. 1, January 2011.
[2] D. L. H. Aik, etc 1, "Power Stability Analysis of Multi-Infeed HVDC Systems", IEEE Transactions on Power Delivery, Vol. 13, No. 3, July 1998.
[3] D.L.H. Aik, etc 1, "Voltage Stability Analysis of Multi-Infeed HVDC Systems", IEEE Tiransactions on Power Delivery, Vol. 12, No. 3, July 1997.
[4] C. K. Kim, etc 4, HVDC Transmission, IEEE & Wiley, 2009.
[5] Guide for Planning DC Links Terminating at AC Systems Locations Having Low Short-Circuit Capacities Part I : AC/DC Interaction Phenomena, Cigre, 1992.
[6] Cheju-Jindo HVDC #2 manual, Alstom, 2010.

Chan-Ki Kim He obtained his M.Sc. and Ph.D. degrees in Electrical Engineering from Chung-Ang University, Korea in 1993 and 1996, respectively. Since 1996, he has been with KEPRI, the R&D center of KEPCO (Korea Electric Power Corporation). His research interests are HVDC, Power Electronics and Generator Control.

Gilsoo Jang He received his M.S. and Ph.D. from Korea University in 1994 and Iowa State University in 1997, respectively. Currently, he is a professor of the School of Electrical Engineering, Korea University. His research interests are power quality and power system control.